



**Acceleration of an Initially Moving Projectile:
Velocity-Injected Railguns and Their Effect
on Pulsed Power**

by Miguel Del Güercio and Alexander Zielinski

ARL-TR-4892

July 2009

NOTICES

Disclaimers

The findings in this report are not to be construed as an official Department of the Army position unless so designated by other authorized documents.

Citation of manufacturer's or trade names does not constitute an official endorsement or approval of the use thereof.

Destroy this report when it is no longer needed. Do not return it to the originator.

Army Research Laboratory

Aberdeen Proving Ground, MD 21005-5066

ARL-TR-4892

July 2009

Acceleration of an Initially Moving Projectile: Velocity-Injected Railguns and Their Effect on Pulsed Power

**Miguel Del Güercio and Alexander Zielinski
Weapons and Materials Research Directorate, ARL**

REPORT DOCUMENTATION PAGE			Form Approved OMB No. 0704-0188		
Public reporting burden for this collection of information is estimated to average 1 hour per response, including the time for reviewing instructions, searching existing data sources, gathering and maintaining the data needed, and completing and reviewing the collection information. Send comments regarding this burden estimate or any other aspect of this collection of information, including suggestions for reducing the burden, to Department of Defense, Washington Headquarters Services, Directorate for Information Operations and Reports (0704-0188), 1215 Jefferson Davis Highway, Suite 1204, Arlington, VA 22202-4302. Respondents should be aware that notwithstanding any other provision of law, no person shall be subject to any penalty for failing to comply with a collection of information if it does not display a currently valid OMB control number. PLEASE DO NOT RETURN YOUR FORM TO THE ABOVE ADDRESS.					
1. REPORT DATE (DD-MM-YYYY) July 2009		2. REPORT TYPE Final		3. DATES COVERED (From - To) March 2009–April 2009	
4. TITLE AND SUBTITLE Acceleration of an Initially Moving Projectile: Velocity-Injected Railguns and Their Effect on Pulsed Power			5a. CONTRACT NUMBER		
			5b. GRANT NUMBER		
			5c. PROGRAM ELEMENT NUMBER		
6. AUTHOR(S) Miguel Del Güercio and Alexander Zielinski			5d. PROJECT NUMBER AH80		
			5e. TASK NUMBER		
			5f. WORK UNIT NUMBER		
7. PERFORMING ORGANIZATION NAME(S) AND ADDRESS(ES) U.S. Army Research Laboratory ATTN: RDRL-WMB-D Aberdeen Proving Ground, MD 21005-5066			8. PERFORMING ORGANIZATION REPORT NUMBER ARL-TR-4892		
9. SPONSORING/MONITORING AGENCY NAME(S) AND ADDRESS(ES)			10. SPONSOR/MONITOR'S ACRONYM(S)		
			11. SPONSOR/MONITOR'S REPORT NUMBER(S)		
12. DISTRIBUTION/AVAILABILITY STATEMENT Approved for public release; distribution is unlimited.					
13. SUPPLEMENTARY NOTES					
14. ABSTRACT Calculations are performed for an initially moving projectile and a railgun. The initial velocity is provided by a 26-mm-diameter conventional propellant gun. A plasma armature is assumed for the railgun. The capacitor-based, pulsed power supply (PPS), located at barricade C, Aberdeen Proving Ground, MD, is assumed to provide the electrical energy for boosting the velocity to 2.5 km/s. Various scenarios are examined with respect to electrical pulse shape, the effect on stored electrical energy, and its distribution in the railgun. Three types of comparisons are used to illustrate the effect of injection velocity on stored electrical energy: efficiency, peak loads, and energy storage. Examples for each category are presented, illustrating complementary areas for propellant gun and railgun operation. Results are promising; however, the initial velocity must be considered in detailed simulations in order for any advantages to be realized.					
15. SUBJECT TERMS railgun, armature, pulsed power, propellant gun					
16. SECURITY CLASSIFICATION OF:			17. LIMITATION OF ABSTRACT	18. NUMBER OF PAGES	19a. NAME OF RESPONSIBLE PERSON
a. REPORT	b. ABSTRACT	c. THIS PAGE			Miguel Del Güercio
Unclassified	Unclassified	Unclassified	UU	30	19b. TELEPHONE NUMBER (Include area code) 410-278-3889

Contents

List of Figures	iv
List of Tables	v
1. Introduction	1
2. Conventional Gun	2
3. Electromagnetic Gun	5
4. Results	7
4.1 Efficiency Perspective.....	7
4.2 Peak Load Perspective.....	12
4.3 Stored Electrical Energy Perspective	15
5. Conclusions	16
6. References	18
Distribution List	20

List of Figures

Figure 1. Photograph of short-slug launch package (12-g sabot/obturator, 46-g slug, 58-g total).....	2
Figure 2. Measured and calculated maximum case mouth pressure for two launch masses.	3
Figure 3. Measured and calculated velocity for two launch masses.....	3
Figure 4. Stored energy reduction for an injected railgun.	8
Figure 5. Railgun efficiency (107 g to 2.5 km/s).....	9
Figure 6. Energy distribution in a railgun (107 g to 2.5 km/s).	9
Figure 7. Railgun currents for 107 g to 2.5 km/s.	10
Figure 8. Stored energy reduction for 10- μ H inductors in the PPS.....	11
Figure 9. Energy distribution in a railgun for 10- μ H inductors in the PPS.	11
Figure 10. Peak railgun current as a function of injection velocity.....	13
Figure 11. Peak barrel pressures (railgun and conventional gun) as a function of injection velocity provided by the conventional gun (single-peak current waveshape).....	13
Figure 12. Peak barrel pressures (railgun and conventional gun) as a function of injection velocity provided by the conventional gun (nearly flat current waveshape).....	14
Figure 13. Optimum injection velocity (equal railgun and conventional gun pressures).....	14
Figure 14. Stored electrical energy as a function of injection velocity.	16

List of Tables

Table 1. Fitting coefficients for 37/26-mm smoothbore cannon and M30 7-P, 0.022-in web propellant (pressure in ksi, velocity in m/s).....	4
Table 2. Peak chamber pressures in conventional gun (ksi).....	4
Table 3. Charge mass (g) required for velocities listed in table 2.	4
Table 4. Comparison of fitted peak chamber pressure to measured data (ksi).....	5
Table 5. Simulation results for peak current and charge voltage (single-peak current pulse).....	6
Table 6. Simulation results for a nearly flat current pulse (not all modules used).	7
Table 7. Results of simulations using 10- μ H inductors for the PPS at barricade C.	11

INTENTIONALLY LEFT BLANK.

1. Introduction

In the early 1980s, the principal mission for railguns required launch velocities in excess of 3 km/s. The focus of the research was centered on railguns employing plasma armatures. Significant efforts were expended on understanding the fundamentals of plasma armatures and their interaction with the bore. The temperatures associated with plasma armatures in railguns typically exceed 2 eV and, as a result, cause significant degradation in the bore materials leading to degradation of railgun performance. One parameter that seemed to ameliorate the effect of long dwell time was the use of a projectile injected into the breech of the railgun. This technique was often used with inert gas as the propulsive media. However, propellants were evaluated (1) and used to inject propellant-accelerated projectiles into the breech of a railgun (2). The burning propellant gases were insufficiently conductive to break down and form a plasma arc with 6000 V applied across the breech of the railgun. While no deleterious interactions were noted between the combustion products and plasma electrodynamics, the research was plagued with large variability in the injection velocity, obturation in the squarebore railgun, and reliable initiation of the plasma. All challenges were eventually solved.

More recently, the mission for railguns has found utility using velocities <3 km/s, thereby avoiding the penalties associated with lossy, high-temperature plasmas. Instead, solid armatures, which were encumbered with other challenges, are now readily employed, particularly those associated with achieving a long bore life and reducing parasitic mass in the launch package.

To a lesser degree, progress has also been made with regard to the energy density of pulsed power sources that are needed to energize railguns. However, the size of military platforms for tactical missions has decreased making it challenging to demonstrate a current, feasible, relevant system.

One option to alleviating the size constraints placed on the pulsed power source (PPS) is to supply a portion of the projectile's kinetic energy through the use of a conventional propellant. To first order, a projectile with one-half of its final kinetic energy at the breech of a railgun would only need to be boosted to attain its final kinetic energy state with a PPS roughly one-half in stored energy capacity (or size).

This report examines a notional railgun injected by a conventional gun with a projectile having an initial velocity. The capacitor-based PPS, located at barricade C, Aberdeen Proving Ground, MD, is assumed to provide the electrical energy for boosting the velocity to 2.5 km/s. Various scenarios are examined with respect to electrical pulse shape, the effect on stored electrical energy, and its distribution in the railgun. In section 2, the propellant gun is assessed from existing experimental data. In section 3, circuit analysis is used to model the railgun with a

launch mass and initial velocity. Operating parameters are derived from the circuit analysis. The results are discussed in section 4, and the conclusions are summarized in section 5.

2. Conventional Gun

The PPS at barricade C is best coupled to a medium-caliber railgun, accelerating on the order of 100 g to hypervelocity (100s kJ). A 26-mm-diameter smoothbore conventional gun was used to accelerate cylindrical slugs fabricated from aluminum into concrete targets (3). Tests were conducted at velocities up to 2223 m/s for a 46-g slug and 1462 m/s for a 92-g slug. The gun was 3 m (10 ft) long and had a maximum pressure rating of 689 MPa (100 ksi). The barrel was chambered for the obsolete U.S. 37-mm cartridge case. The bore diameter was reduced to (nominally) 26 mm ahead of the case mouth. A full cartridge case holds 300 g of propellant mass, although it is possible to fit an additional 15 g in the case. Propellant M30 7-P, 0.022-in Web, and MK22 MOD L70 Primer were used for these experiments.

The aluminum slug requires an obturator to create a pressure seal for the expanding propellant gases and a sabot to ride along the inner bore surface. Polypropylux 944 (Westlake Plastic) is a tough and rubbery polypropylene-based plastic and was used to fabricate the obturator/sabot. The forward section of the sabot was grooved, 3×3 mm ($1/8 \times 1/8$ in), at a minor diameter of 26 mm (1.022 in) to provide a volume into which the plastic could flow without generating extreme hydrostatic pressures between the aluminum slug and the inside surface of the bore. A picture of the short-slug launch package is shown in figure 1 (58-g total).

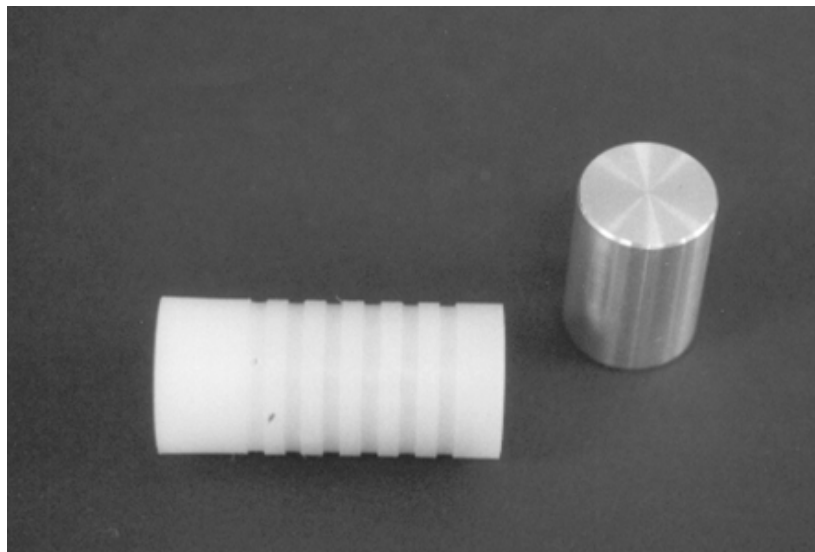


Figure 1. Photograph of short-slug launch package (12-g sabot/obturator, 46-g slug, 58-g total).

Figure 2 shows a plot of the maximum case mouth pressure for the test series with two launch masses (58 and 107 g) (3). The solid and dashed lines in the plot are for simulations conducted prior to the test series using the interior ballistics code IBHVG2 (4). The calculations consistently overestimate the measured values. The significant deviation for charge mass <200 g between the experimental data and the theoretical calculations was presumed to occur because not all the propellant was burned during launch package acceleration. In fact, unburned propellant was noticed 1 to 2 m downrange on the x-ray cassette. A similar plot for the launch package velocity is shown in figure 3 (3).

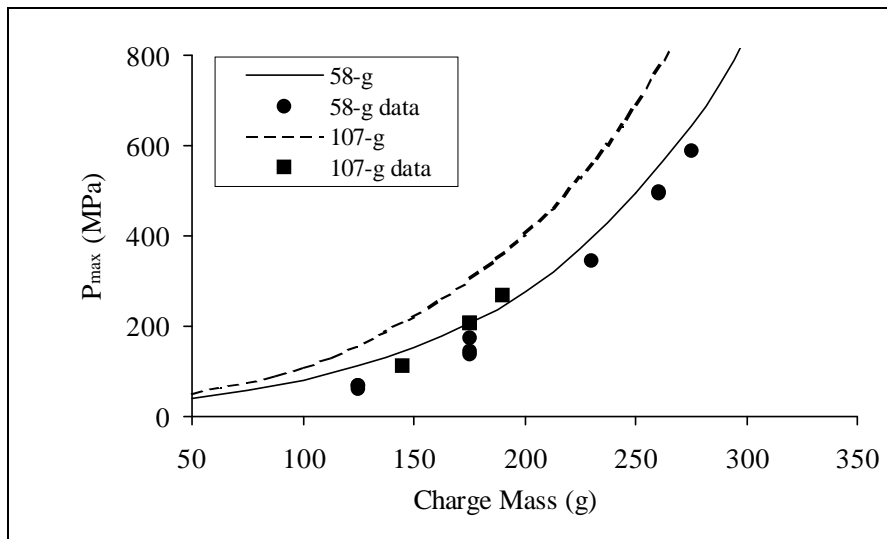


Figure 2. Measured and calculated maximum case mouth pressure for two launch masses (3).

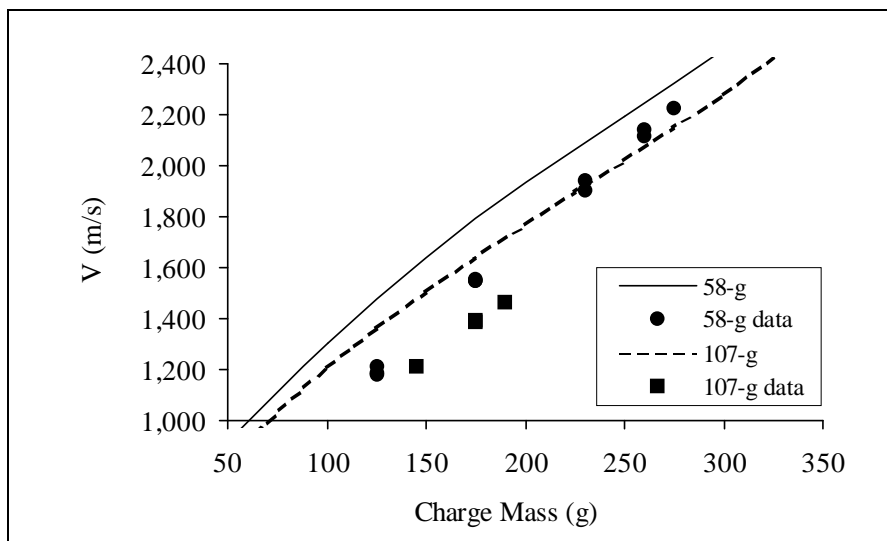


Figure 3. Measured and calculated velocity for two launch masses (3).

For the purpose of this report, it was more convenient to fit the measured data for the 58- and 107-g launch packages using equation

$$F = C1(x)^n, \tag{1}$$

where x is the charge mass in grams, and F is either the peak chamber pressure (in ksi) or exit velocity (in m/s), depending on the coefficients $C1$ and n . Additionally, the data was extrapolated to a third launch mass (150 g) in order to perform calculations over the full extent of possibilities utilizing the PPS at barricade C. Table 1 provides the fitting coefficients.

Table 1. Fitting coefficients for 37/26-mm smoothbore cannon and M30 7-P, 0.022-in web propellant (pressure in ksi, velocity in m/s).

Launch Mass (g)	Coefficients	$F = \text{Peak Chamber Pressure}$	$F = \text{Exit Velocity}$
58	n	2.78	0.79
	$C1$	1.4E-05	26.0
107	n	3.18	0.70
	$C1$	2.1E-06	37.4
150	n	3.53	0.62
	$C1$	5.00E-07	47.4

Using the coefficients provided in table 1, a table of peak chamber pressure can be generated to obtain velocities injected into the breech of the railgun for the launch masses indicated in table 1. Table 2 lists the peak chamber pressures for three exit velocities (railgun injection velocities), 1.0, 1.5, and 2.0 km/s.

Table 2. Peak chamber pressures in conventional gun (ksi).

Velocity (km/s)	58 g	107 g	150 g ^a
1.0	5	7	17
1.5	22	40	167 ^b
2.0	61	150 ^b	872 ^b

^aExtrapolated from measured data (3).

^bUnrealistic but included for completeness.

Table 3 lists the amount of propellant (i.e., charge mass) needed to achieve the velocities indicated in table 2.

Table 3. Charge mass (g) required for velocities listed in table 2.

Velocity (km/s)	58 g	107 g	150 g
1.0	100	110	135
1.5	170	195	260
2.0	245	295	415

The fit was checked against measurements made for the 58- and 107-g tests where applicable (estimates for a launch mass of 150 g are extrapolated from 58- and 107-g data and therefore no comparison to data are possible). The comparisons for chamber pressure are listed in table 4. It can be seen that the estimates are in good agreement with the measured data.

Table 4. Comparison of fitted peak chamber pressure to measured data (ksi).

Nominal Velocity (km/s)	58 g Measured	Fit (equation 1)	107 g Measured	Fit (equation 1)
1.5	25	24	39	38
2.0	50	51	NA	NA

Note: NA = not applicable.

3. Electromagnetic Gun

To date, very little work has been done on solid armatures injected into a railgun (5). The results have not been promising. Solid armatures operated in this manner experienced transition to arcing contacts almost immediately upon engaging the rails. It is likely that the coupled electrostatics and mechanical dynamics are not straightforward and could present a significant challenge, particularly when the injection velocity exceeds 1 km/s. Also challenging is the load management on the contacts of the solid armature when the current is low and rising. The most successful armature designs utilize an initial interference fit between the armature contact and the rail as well as the force created by the interaction of the current and magnetic induction field to apply the contact of the armature against the rail. This regime of operation is called start-up. An armature contact that does not perform well during start-up has increased Ohmic losses, is not known to recover to a less lossy state, produces increased damage to the bore, and damages the flight vehicle. When the aforementioned are combined with a solid armature coexisting in the environment of a propellant gun (e.g., high temperature and pressure), it is likely that the parasitic mass will have to increase compared to the all-electric solution (i.e., increased kinetic energy losses).^{*} The shape of the current pulse has a pronounced effect on railgun performance when a solid armature is used (6). A single-peak waveform caused the solid armature to lose metal-on-metal contact (i.e., transition) for the shortest length of travel; thereafter, the Ohmic losses from the armature continued to grow, albeit at a lower magnitude than that of a full-bore plasma armature.

On the other hand, plasma armatures are relatively simple for the operational parameters under consideration in this study. The assumed railgun is based on a smooth (physical) transition from the 26-mm smoothbore conventional cannon.^{*}

^{*} Conceivably, the operational nature of the conventional gun and railgun can be combined into a single barrel, with the propulsive media comingled. The basic conclusions related to the present study are not expected to significantly change. However, additional detailed engineering is required for further evaluation and is beyond the scope of the present study.

Using a plasma armature in a 26-mm roundbore railgun will generate an Ohmic-loss term for the armature of roughly 220 V at a current of about 400 kA (7–10). The voltage drop across the plasma armature is dependent on the current conducted through the plasma armature; at <400 kA, the drop is estimated to be about 200 V, and at >400 kA, the drop is roughly 350 V.* Obturation based on conventional propellant-gun technology has been successfully demonstrated in large-caliber plasma armature railguns launching tactical-like payloads in both base-push and mid-ride sabot topologies (11). The obturator shown in figure 1 would suffice for sealing the plasma armature under consideration in this study. Finally, initiation of the plasma armature has been successfully demonstrated for initially moving (2) and stationary (11) projectiles.

All pulsed power supplies have a finite-duration rise time. For railguns, fast rise times can present challenges with regards to rapid, repetitive switching of solid-state devices (12) and damaging stress-wave amplification in structural elements of projectiles (13).

When the initial velocity is >0, the velocity increases very little when the current is low and rises toward its peak value. For example, in the case where the injection velocity is 2 km/s, during the rise time of the current pulse from the PPS at barricade C (0.8 ms), the projectile will consume roughly 1.4 m of the length of the railgun (ignoring friction and drag). The railgun currently in operation at barricade C provides for 2.67 m of projectile travel. Clearly, very little increase in velocity would occur for reasonable peak currents. Therefore, the calculations for the railgun and the PPS performance at barricade C were carried out using the electrical simulation code SPICE (14, 15). Two waveshapes for the current pulse are examined: a single-peak shape and a nearly flat shape. Both shapes have finite rise and decay times. The railgun is assumed to be a 26-mm-diameter plasma armature railgun with a length of 4 m. The cross-sectional area of the bore, used to determine velocity retardation due to the compression of the air column resident in the bore of the railgun, which is significant for velocities >2 km/s, is 530 mm². Finally, the rails are assumed to be fabricated from a low-conductivity, high-strength copper alloy. All exit velocities from the railgun are 2.5 km/s.

For a current pulse that has a single peak, all the modules are triggered to discharge at time = 0. Results from the simulations are listed in table 5, considering three launch masses and four injection velocities.

Table 5. Simulation results for peak current and charge voltage (single-peak current pulse).

Injected Velocity (km/s)	58 g		107 g		150 g	
	(kA)	(kV)	(kA)	(kV)	(kA)	(kV)
0.0	751	5.65	998	7.4	1180	8.7
1.0	592	4.85	790	6.4	931	7.5
1.5	497	4.25	658	5.5	775	6.5
2.0	391	3.50	511	4.5	600	5.25

*Using a solid armature does not preclude losses. Unless completely integrated into the flight vehicle, the mass offered by the solid armature is a loss term. The real metric should be the bore damage and barrel lifetime. Both solid armatures and plasma armatures cause damage to the insulator and conductors of a railgun.

For the nearly flat current shape, the charge voltage and time delays for triggering each module in the PPS are adjusted in order to remain below the peak currents listed in table 6 and still achieve an exit velocity of 2.5 km/s.

Table 6. Simulation results for a nearly flat current pulse (not all modules used).

Injected Velocity (km/s)	58 g		107 g		150 g	
	(kA)	(kV)	(kA)	(kV)	(kA)	(kV)
0.0	486	7.25	629	9.25	752	11.0
1.0	464	7.25	621	9.5	741	11.5
1.5	424	6.75	562	8.75	678	10.5
2.0	352	5.75	453	7.25	562	9.0

4. Results

The simulation results can be assessed many ways. In the following subsections, three perspectives are presented to assess the effectiveness of the system. In the first subsection, the electrical efficiency is discussed as it ultimately has a major impact on managing the resultant thermal loads. In the next subsection, the peak mechanical loads from the conventional propellant gun and railgun are considered. In the last subsection, the merits of injection are discussed relative to stored electrical energy.

4.1 Efficiency Perspective

Figure 4 shows a plot of the reduction of stored electrical energy as a function of the portion of final muzzle kinetic energy supplied by the conventional gun. The origin represents the all-electric case. The black solid line represents “breakeven,” where the percentage of the final kinetic energy supplied by the railgun is equal to the percentage of electrical energy reduced from the all-electric operating condition. Operating below the line is less efficient. For example, for the nearly flat pulse shape, supplying 20% of the final muzzle kinetic energy from the conventional gun reduces the stored electrical energy by 16%. All pulse shapes considered provide for a reduction in stored electrical energy (as compared to the all-electric case). However, the extent of the reduction is dependent on a number of considerations. None of the nearly flat pulses considered in this study reach breakeven (although the amount of stored electrical energy is less than that required for an all-electric solution). The single-peak solutions achieve breakeven when the conventional gun provides up to 60% of the final muzzle kinetic energy. If the conventional gun provides more than 60% of the kinetic energy (>2 km/s), the railgun is less efficient at converting the electrical energy to kinetic energy.

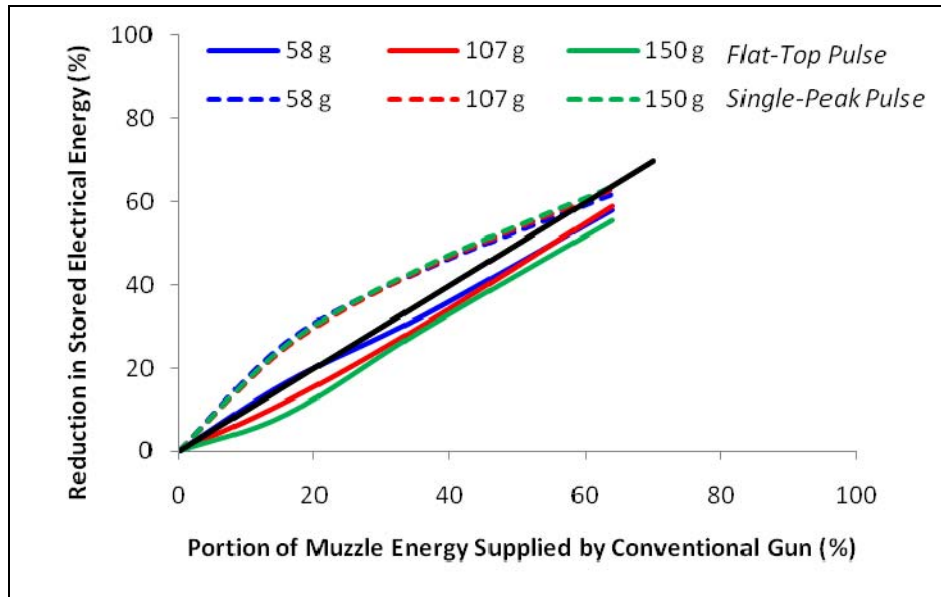


Figure 4. Stored energy reduction for an injected railgun.

It is also instructive to look at the various energy terms in a railgun and how they are influenced by the inclusion of a nonzero initial velocity. The primary energy terms in a railgun are the kinetic energy, Ohmic losses, and magnetic energy. The Ohmic losses are those associated with the voltage drop across the breech, rails, and armature, each multiplied by the current and integrated over time. The magnetic energy is also associated with the breech and rails (armature inductance is assumed to be negligible) and is one-half the inductance multiplied by the square of the current. The summation of these terms at any given time during the launch is the energy delivered to the breech of the railgun.

An example is presented which focuses on the effect of the injection velocity: nonexistent (0 m/s), more efficient (1 km/s), and then least efficient (2 km/s). Energy distribution in the railgun is examined for the 107-g launch mass operated with a single-peak current pulse.

The electrical efficiency of the railgun, shown in figure 5, reveals a decrease in efficiency at the time of exit for a range of injection velocities (1–2 km/s).

In order to ascertain the exact cause of the reduction, the individual components of energy in the railgun, plotted in figure 6 for three different injection velocities, are examined relative to the amount of electrical energy delivered to the breech.

As expected, the relative contribution of energy to the Ohmic losses for the armature, rails, and breech decreases as the injection velocity is increased, owing to the reduced in-bore residence time as well as significantly lower currents. However, the relative contribution to the stored magnetic energy residing in the breech and rails when the projectile exits the railgun is increasing. The current delivered from the PPS at barricade C is not designed to rapidly decay

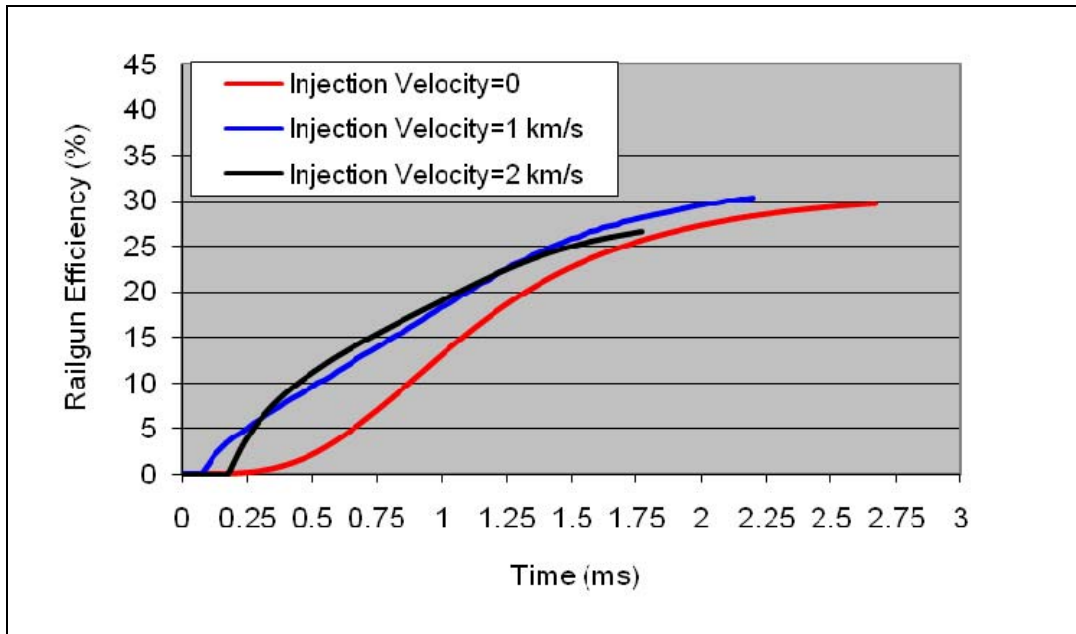


Figure 5. Railgun efficiency (107 g to 2.5 km/s).

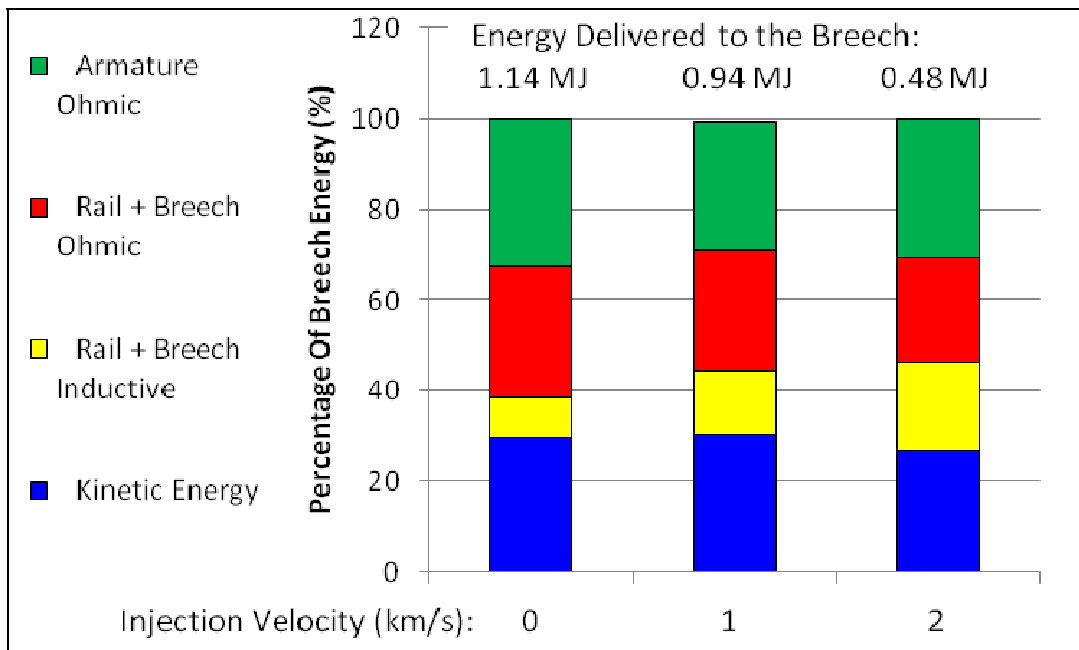


Figure 6. Energy distribution in a railgun (107 g to 2.5 km/s).

prior to the projectile exiting the railgun (in fact, solid-armature railguns function best for nearly flat current waveshapes [6]). Relatively large currents at exit become more pronounced as the injection velocity is increased and, consequently, the in-bore residence time is reduced. This effect also becomes more evident when the nearly flat current waveshape is used since the current has even less time to decay prior to projectile exit. For completeness, the corresponding currents are shown in figure 7, plotted as a function of time.

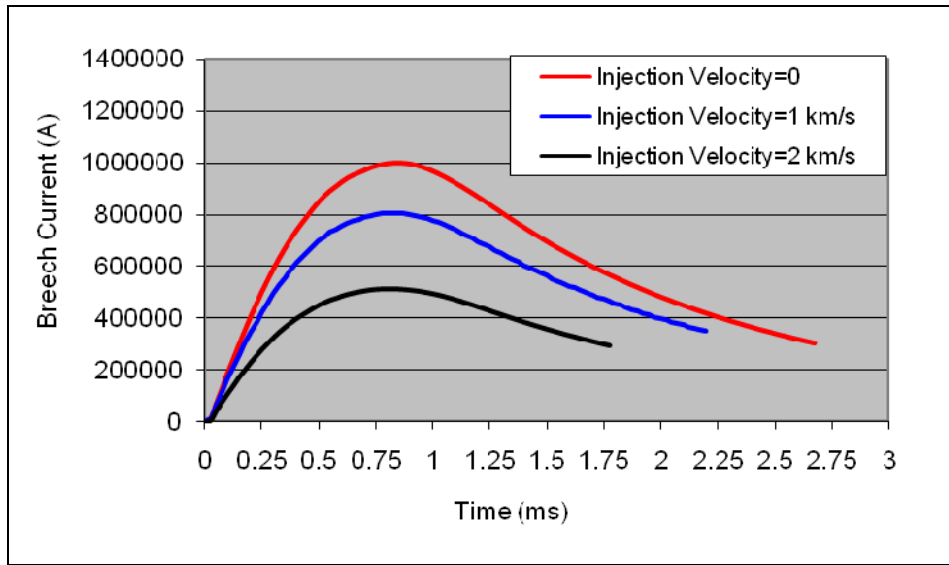


Figure 7. Railgun currents for 107 g to 2.5 km/s.

In an attempt to better match the time scale of the current pulse to the in-bore residence time, the inductors of the PPS were arbitrarily reduced to 10 μH in the simulation. The reduced value will shorten the time to reach peak current as well as hasten the decay after peak current. The resistances for each of the inductors were left unchanged. All modules were used. The time to reach peak current is nominally 0.3 ms (as compared to 0.8 ms when utilizing the PPS and original inductors).

Table 7 lists the simulation results. As expected, the peak current necessary to achieve 2.5 km/s from the railgun has increased as compared to the corresponding cases where the PPS was used with their original inductors. However, with the 10- μH inductors producing a more suitable time scale, the efficiency has increased, most notably for an injection velocity of 1 km/s (supplying 16% of the final muzzle kinetic energy now yields a 30% reduction in stored energy) and also somewhat increased at an injection velocity of 2 km/s (supplying 64% of the final muzzle kinetic energy yields a 68% reduction in the stored energy). These results are illustrated by the plot shown in figure 8. Clearly, the design of a pulsed power source must account for the initial velocity in order to take advantage of any potential gains in efficiency. These gains are also clearly seen when illustrating the distribution of energy in the railgun as shown in the plot of figure 9.

Table 7. Results of simulations using 10- μ H inductors for the PPS at barricade C.

Injection Velocity (km/s)	Peak Current (kA)	Charge Voltage (kV)
0.0	1390	7.1
1.0	1050	5.95
2.0	634	4.0

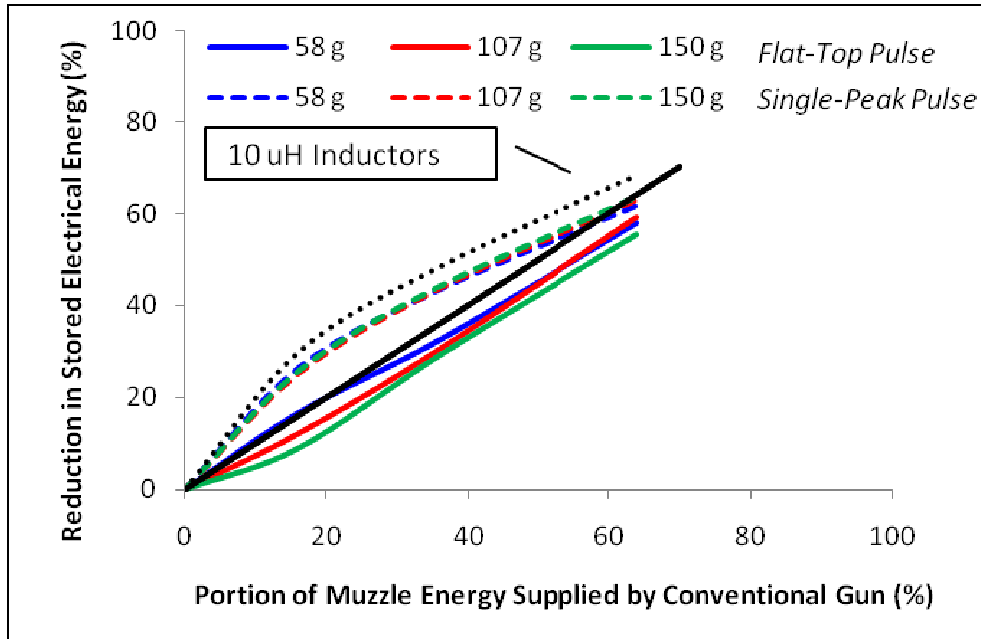


Figure 8. Stored energy reduction for 10- μ H inductors in the PPS.

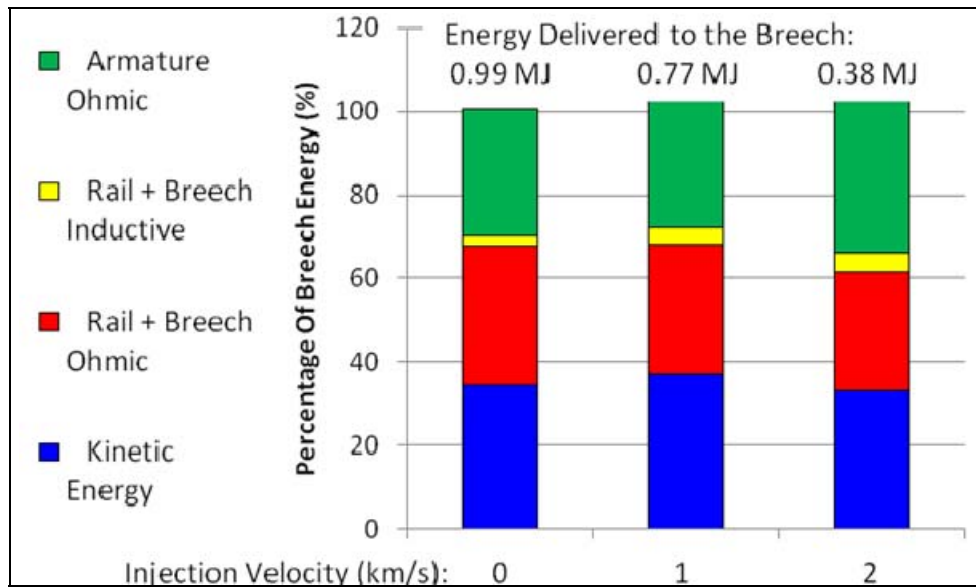


Figure 9. Energy distribution in a railgun for 10- μ H inductors in the PPS.

Finally, a case is considered to examine the sensitivity of the simulations to the armature voltage. One of the highest peak currents considered in this study is used (998 kA), which corresponds to the case of 107 g with no injection velocity and a single-peak current pulse. Using the simulation results from table 5, a 1-MA current is estimated to produce an armature voltage of ~375 V. The simulation was repeated using 375 V for the plasma armature voltage drop. The peak current remained approximately the same for the 220-V drop (998 vs. 1020 kA), but the charge voltage and breech energy increased from 7.4 to 7.75 kV and from 1.14 to 1.37 MJ, respectively, in order to account for the additional loss. Further analyses for the remaining cases are not expected to reveal any significant changes to the conclusions.

4.2 Peak Load Perspective

The peak current required to achieve an exit velocity of 2.5 km/s from the railgun can also be a factor affecting the semiconductor switches in a PPS and breech and launcher structural requirements; the management of large peak currents places challenges on efficient mechanical design in order to control Ohmic losses.

The peak current needed to produce an exit velocity of 2.5 km/s from the railgun is plotted as a function of injection velocity in figure 10. The peak current for a single-peak waveshape is continuously reduced as the injection velocity is increased. However, no reduction in peak current is evident for a nearly flat shape when the injection velocity is <50% of the final velocity. This effect is attributed to the aforementioned inability of the PPS to match the electrical time scale of the current to the in-bore residence time.

Finally, it is also instructive to compare the peak pressures between the conventional gun and the railgun. Since peak pressure usually determines the structure of the projectile, it seems reasonable to maintain the same structure for both systems. Bear in mind that the length of the gun and injection and/or exit velocity is also determined by the peak pressure. The peak pressure for the railgun is calculated from the Lorentz force:

$$P_{pk} = \frac{\frac{1}{2} L' I_{pk}^2}{\pi r^2}, \quad (2)$$

where L' is the inductance gradient of the railgun assumed to be 0.45 $\mu\text{H/m}$ and r is the radius of the bore, taken to be 13 mm. The peak barrel pressures for the conventional gun and railgun are shown in figures 11 (single-peak current) and 12 (nearly flat current).

The pressure for the railgun is proportional to the current squared. Also as expected, the pressure in the conventional gun increases dramatically as the velocity increases. An optimum injection velocity, shown plotted in figure 13, can be found from the intersection of the conventional gun and railgun pressure curves.

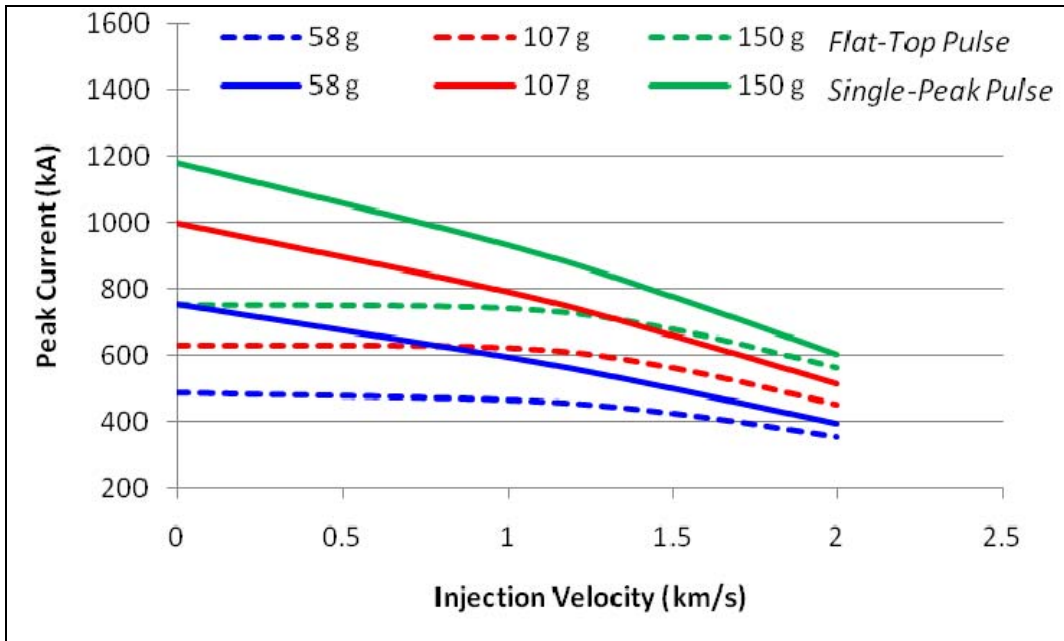


Figure 10. Peak railgun current as a function of injection velocity.

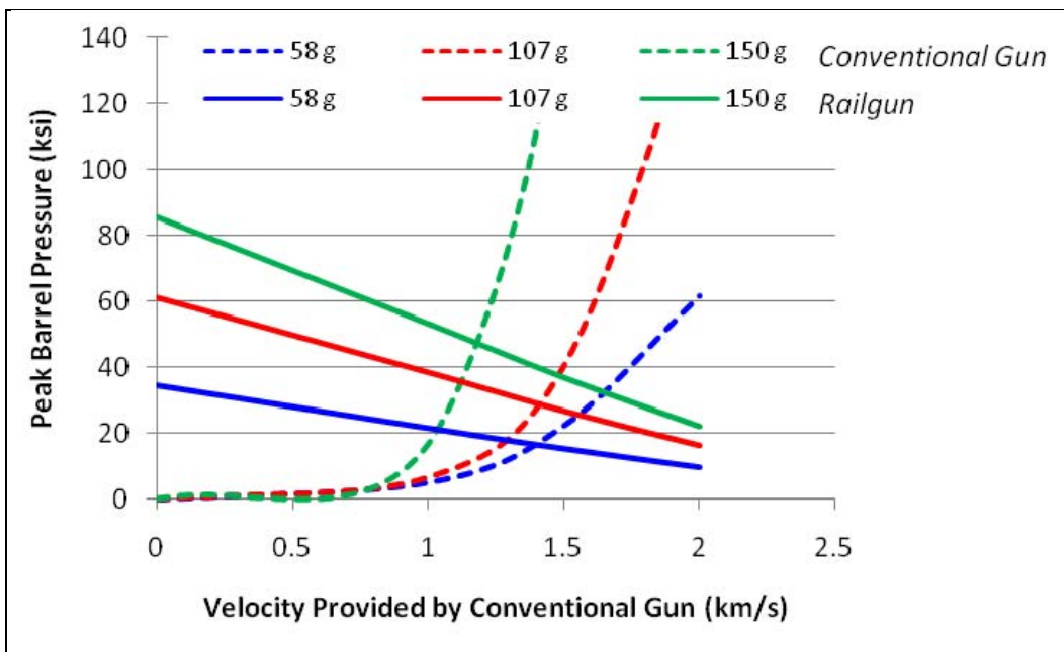


Figure 11. Peak barrel pressures (railgun and conventional gun) as a function of injection velocity provided by the conventional gun (single-peak current waveshape).

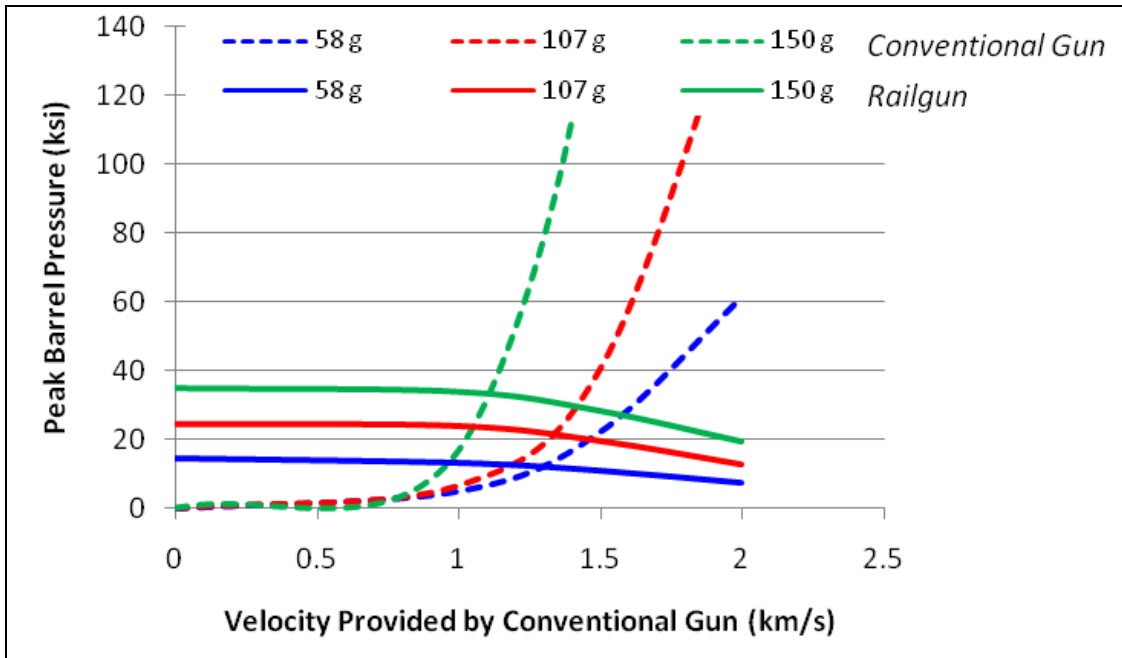


Figure 12. Peak barrel pressures (railgun and conventional gun) as a function of injection velocity provided by the conventional gun (nearly flat current waveshape).

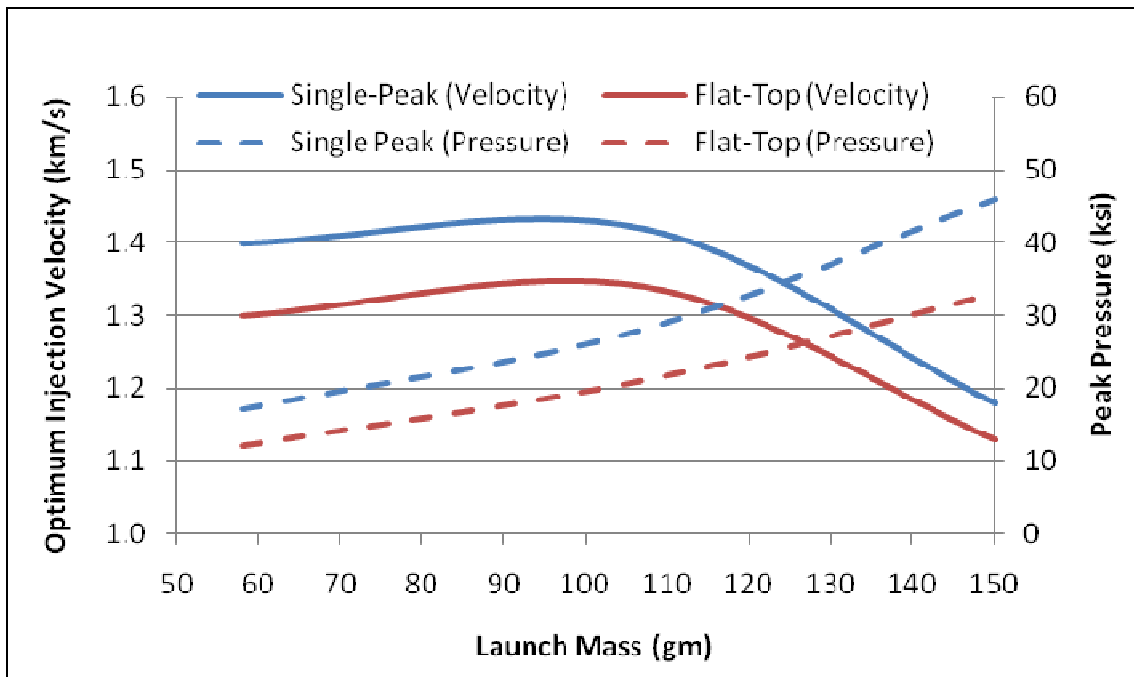


Figure 13. Optimum injection velocity (equal railgun and conventional gun pressures).

For the system under consideration, the optimum injection velocity is roughly 1.35 km/s, regardless of (reasonable) launch mass and shape of the current pulse. Additionally, the peak pressure (for both guns) is quite manageable (i.e., <30 ksi), regardless of (reasonable) launch mass and shape of the current pulse. Figures 11–13 are presented as one example of how system optimization and assessment might be conducted when considering peak loads as the figure of merit. As already mentioned, the dependency of the armature voltage on the currents considered in this study is not expected to cause a significant deviation to the conclusions made relative to peak loads.

4.3 Stored Electrical Energy Perspective

Another possible trade solely involves the amount of stored electrical energy. If sources of available pulsed power are limited, then issues of electrical efficiency and projectile structural efficiency become second-order considerations.

If, for example, size and weight preclude stored electrical energy >2 MJ, then using the systems discussed in this study, a number of options are available to reach 2.5 km/s with a 107-g mass; two options found in figure 14 are to inject the projectile into the railgun at ~1.7 km/s and use a nearly flat current pulse or inject at ~0.7 km/s and use a single-peak waveshape. While using a conventional gun to provide an initial velocity offers flexibility in stored electrical energy, care must be taken with the mechanical integrity of the guns as the peak chamber pressure for the conventional gun, providing 1.7 km/s of initial velocity, is rather high (75 ksi) and moderately high for the railgun with an initial velocity of 0.7 km/s (~45 ksi).

Significant reductions in stored electrical energy begin to appear when the injection velocity is greater than roughly 1.3 km/s. For example, as illustrated in figure 14, accelerating a 107-g launch mass to 2.5 km/s with a nearly flat current pulse requires 3.5 MJ with no initial velocity vs. 3.0 MJ with an injection velocity of 1 km/s (an inconsequential decrease in stored electrical energy for integrating the large burden of a second, different system [i.e., propellant gun]). However, at 1.7 km/s, the stored electrical energy is significantly reduced to 2 MJ. The consideration of armature voltage as a function of current most significantly affects the stored energy when the current is the largest, which occurs for very low injection velocities. The effect in the plot shown in figure 14 would be a slight but perceptible increase in the amount of stored electrical energy near the abscissa but inconsequential as the injection velocity is increased. With no injection velocity, the 107-g mass would require a stored energy of 2240 kJ for the 220-V drop and 2450 kJ for the 375-V drop.

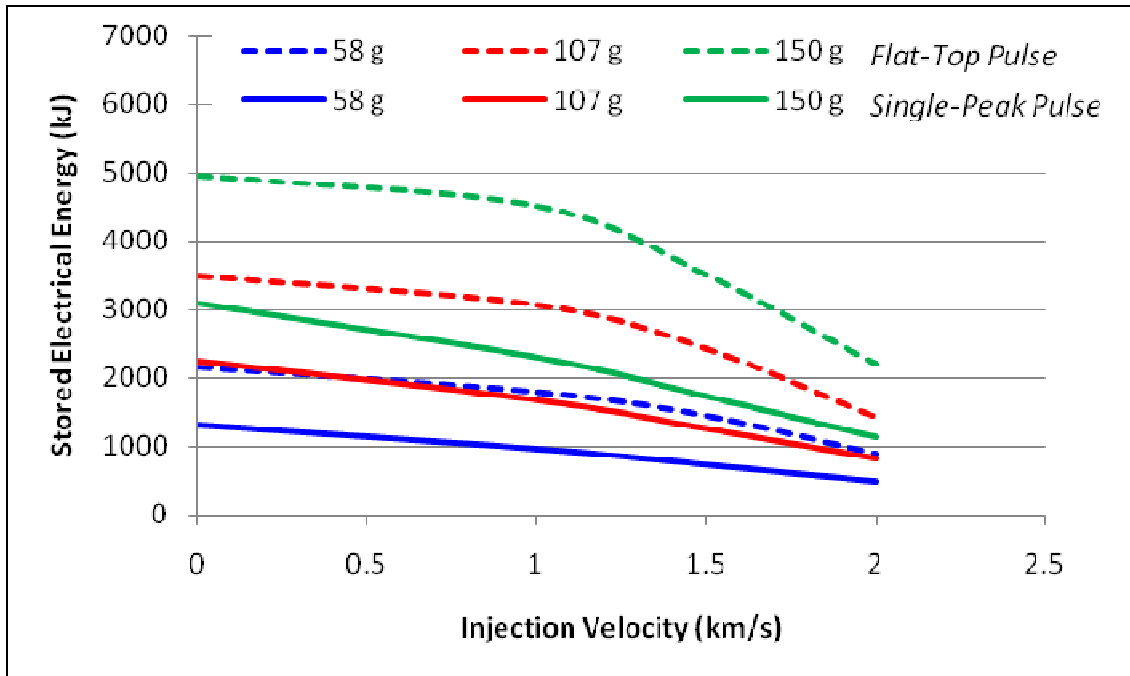


Figure 14. Stored electrical energy as a function of injection velocity.

5. Conclusions

The study presented in this report relies on the proven and reliable demonstration of a 26-mm-diameter smoothbore conventional propellant gun. Also, the study assumes use of the PPS at barricade C, a pulsed power supply designed for solid-armature railgun operation. Challenges offered from incorporating a solid-armature railgun injected by a conventional propellant gun are discussed. Furthermore, for demonstrating energy storage reduction, a low-risk alternative is to use a plasma-armature railgun. Electrical circuit simulations were used to assess the performance of a plasma-armature railgun where the initial velocity of the projectile was provided by a conventional propellant gun. The results from the simulations can be assessed in numerous ways.

Three perspectives are presented to assess the effectiveness of the system. In the first case, the electrical efficiency is discussed as it ultimately has a major impact on managing the resultant thermal loads. In all cases considered, the reduction of stored electrical energy was nearly equal to the percentage of kinetic energy supplied by the conventional gun, making this technique attractive for size-limited platforms. The electrical efficiency was somewhat hindered by the use of the PPS at barricade C, largely due to the inductance of each module, which tends to keep the current from rapidly decaying after attaining its peak value. This deficiency also affected the use of a nearly flat current pulse shape. Improvement in the efficiency resulted when the inductance

was decreased and highlights the need for detailed pulsed-power simulations for nonzero initial velocity. Additionally, the finite rise time of the current pulse necessitated the use of a 4-m-long railgun. The most efficient initial velocity appears to be in the 1- to 1.5-km/s range.

In the second case, the peak mechanical loads from the conventional propellant gun and railgun are considered. The presence of an initial velocity tends to reduce the peak current, thereby reducing the peak pressure in the railgun barrel. Peak chamber pressure in the conventional gun tends to increase for large exit velocities. Optimizing for equal pressure in both gun systems yields an optimum injection velocity of 1.35 km/s.

Finally, in the last case, the merits of injection are discussed relative to stored electrical energy. Significant reduction in stored energy is realized (~50%) when the injection velocity is >1.7 km/s.

Using the previously mentioned perspectives and minimizing risk, a very straightforward test series could demonstrate the feasibility and validate the assumptions for accelerating an initially moving projectile. A 100-g, 26-mm-diameter projectile launched into the breech of a railgun at 1.3 km/s with a peak chamber pressure of 25 ksi could be further accelerated to 2.5 km/s with 2–3 MJ of stored electrical energy and a peak current of 600–750 kA using the 5-MJ, capacitor-based PPS located at barricade C.

6. References

1. Chung, M. J. *Initial Acceleration for Electromagnetic Launchers: A Feasibility Study on Chemical Propellants*; MRL-TN-748; Defence Science and Technology Organisation, Materials Research Laboratory: Melbourne, Victoria, 1983.
2. Stainsby, D. F.; Sadedin, D. R. *Experiments With a Small Injected Railgun*; MRL-R-1055; Defence Science and Technology Organisation, Materials Research Laboratory: Melbourne, Victoria, June 1987.
3. Zielinski, A.; Silsby, G. *Hypervelocity Penetration Impacts in Concrete Targets*; ARL-TR-2038; U.S. Army Research Laboratory: Aberdeen Proving Ground, MD, September 1999.
4. Anderson, R.; Fickie, K. *IBHVG2 – A User’s Guide*; BRL-TR-829; U.S. Army Ballistics Research Laboratory: Aberdeen Proving Ground, MD, July 1987.
5. Garner, J.; Zielinski, A.; Jamison, K. Design and Testing of a Mass-Stabilized Projectile for a Small Caliber, Electromagnetic Launcher. *IEEE Transactions on Magnetics* **1989**, 25 (1), 197–202.
6. Del Güercio, M.; Michlin, A.; Zielinski, A. Current Pulse Shape on Armature Contact Performance. Presented at the 22nd Electric Launcher Association (ELA) Meeting 07-09, San Diego, CA, November 2005.
7. Zielinski, A.; Powell, J. *Plasma Analysis of a Small-Bore Arc-Armature Railgun*; BRL-TR-3175; U.S. Army Ballistics Research Laboratory: Aberdeen Proving Ground, MD, November 1990.
8. Jamison, K.; Burden, H. Measurements of Plasma Properties From a Large Bore, Plasma Armature Railgun. *IEEE Transactions on Magnetics* **1989**, 25 (1), 256–261.
9. Jackson, G.; Tower, M.; Haight, C. Scaling Relationships for Plasma Driven Railguns. *IEEE Transactions on Magnetics* **1989**, 25 (1), 252–255.
10. Parker, J. V. An Empirical Model for Plasma Armature Voltage. *IEEE Transactions on Magnetics* **1991**, 27, 283–288.
11. Elder, D. The First Generation in the Development and Testing of Full-Scale, Electric Gun-Launched, Hypervelocity Projectiles. *IEEE Transactions on Magnetics* **1997**, 33 (1), 53–62.
12. O’Brien, H.; Shaheen, W.; Thomas, R.; Crowley, T.; Bayne, S.; Scozzie, C. Evaluation of Advanced Si and SiC Switching Components for Army Pulsed Power Applications. *IEEE Transactions on Magnetics* **2007**, 43 (1), 259–264.

13. Bannister, K.; Burton, L.; Drysdale, W. Structural Design Issues for Electromagnetic Projectiles. *IEEE Transactions on Magnetics* **1991**, 27 (1), 464–469.
14. Del Güercio, M. *A Spice-Based Code for ARL's 4.5-MJ Electromagnetic Launcher Pulsed Power Supply System*; ARL-TR-2592; U.S. Army Research Laboratory: Aberdeen Proving Ground, MD, September 2001.
15. Zielinski, A.; Del Güercio, M.; Michlin, A.; Niles, S.; Canami, A.; Glassman, R. *Incident, Action, Recovery, and Recommissioning for the 4.5-MJ Pulsed Power Supply, Located at the Electromagnetic Gun Facility, Barricade C, Aberdeen Proving Ground, MD*; ARL-TR-4088; U.S. Army Research Laboratory: Aberdeen Proving Ground, MD, April 2007.

NO. OF
COPIES ORGANIZATION

1 DEFENSE TECHNICAL
(PDF INFORMATION CTR
only) DTIC OCA
8725 JOHN J KINGMAN RD
STE 0944
FORT BELVOIR VA 22060-6218

1 DIRECTOR
US ARMY RESEARCH LAB
IMNE ALC HRR
2800 POWDER MILL RD
ADELPHI MD 20783-1197

1 DIRECTOR
US ARMY RESEARCH LAB
RDRL CIM L
2800 POWDER MILL RD
ADELPHI MD 20783-1197

1 DIRECTOR
US ARMY RESEARCH LAB
RDRL CIM P
2800 POWDER MILL RD
ADELPHI MD 20783-1197

ABERDEEN PROVING GROUND

1 DIR USARL
RDRL CIM G (BLDG 4600)

NO. OF
COPIES ORGANIZATION

1 US ARMY MATERIAL COMMAND
AMC DCG T
5001 EISENHOWER BLVD
ALEXANDRIA VA 22333-0001

1 US ARMY MISSILE COMMAND
AMSRD AMR W
W C MCCORKLE
5400 FOWLER RD
REDSTONE ARSENAL AL 35898-5240

1 US ARMY TACOM TARDEC
AMSTA TR D MS 207
M TOURNER
WARREN MI 48397-5000

4 US ARMY TACOM ARDEC
AMSRD AAR AEW E D
M CILLI
D LADD
J BENNETT
S FOSTER
BLDG 382
PICATINNY ARSENAL NJ 07806-5000

1 US ARMY RDECOM ARDEC
BENET LAB
E KATHE
WATERVLIET ARSENAL BLDG 115
1 BUFFINGTON ST
WATERVLIET NY 12189-4000

1 CSSDD NSWC
COMMANDING OFFICER
CODE A76 TECHNICAL LIBRARY
6703 W HWY 98
PANAMA CITY FL 32407-7001

2 OFFICE OF NAVAL RESEARCH
E D'ANDREA CODE 352
R ELLIS CODE 352
875 N RANDOLPH ST
ARLINGTON VA 22203-1995

1 UNIV AT BUFFALO SUNY AB
J SARJEANT
PO BOX 601900
BUFFALO NY 14260-1900

1 SAIC
K JAMISON
PO BOX 4216
FORT WALTON BEACH FL 32542

NO. OF
COPIES ORGANIZATION

2 NAVAL RESEARCH LABORATORY
R MEGER CODE 6750
R HOFFMAN CODE 6750
4555 OVERLOOK AVE SW
WASHINGTON DC 20375-5346

4 NSWC DAHLGREN DIVISION
Q20 J BERNARDES
G30 B MCGLASSON
G308 C GARNETT
G32J POYNOR
17320 DAHLGREN RD
DAHLGREN VA 22448-5100

3 INST FOR ADVANCED TECH
UNIV OF TEXAS AT AUSTIN
I MCNAB
F STEPHANI
T WATT
3925 WEST BRAKER LANE
STE 400
AUSTIN TX 78759-5316

2 UNIV OF TEXAS AT AUSTIN
CENTER FOR ELECT
J KITZMILLER
J PAPPAS
PRC MAIL CODE R7000
AUSTIN TX 78712

2 BAE
B GOODELL
R JOHNSON
MS M170
4800 E RIVER RD
MINNEAPOLIS MN 55421-1498

1 UNIV OF TEXAS AT AUSTIN
M DRIGA
ENS 434 DEPT OF ECE
MAIL CODE 60803
AUSTIN TX 78712

1 SAIC
J BATTEH
4901 OLDE TOWNE PARKWAY
STE 200
MARIETTA GA 30068

1 SAIC
A WALLS
8303 N MOPAC EXPRESSWAY
STE B 450
AUSTIN TX 78759

NO. OF
COPIES ORGANIZATION

- 2 IAP RESEARCH INC
D BAUER
J BARBER
2763 CULVER AVE
DAYTON OH 45429-3723
- 1 TITAN CORPORATION
T WOLFE
4855 RUFFNER ST
STE A
SAN DIEGO CA 92111
- 1 GA ESI
GENERAL ATOMICS ELECTRONIC
SYSTEMS
F MACDOUGALL
4949 GREENCRAIG LANE
SAN DIEGO CA 92123
- 1 NORTH CAROLINA STATE UNIV
DEPT OF NUCLEAR ENGR
M BOURHAM
BOX 7909
RALEIGH NC 27695-7909

ABERDEEN PROVING GROUND

- 10 DIR USARL
RDRL WM
P PLOSTINS
RDRL WMM B
J TZENG
R KASTE
R EMERSON
RDRL WMB D
A ZIELINSKI
A MICHLIN
M DEL GÜERCIO
C CANDLAND
R BEYER
RDRL WMT E
J POWELL